

# IGNITION, TRANSITION, FLAME SPREAD IN MULTIDIMENSIONAL CONFIGURATIONS IN MICROGRAVITY

Takashi Kashiwagi<sup>1</sup>, William E. Mell<sup>1</sup>, Howard R. Baum<sup>1</sup>, Sandra Olson<sup>2</sup>

<sup>1</sup>Mail Stop 8652, National Institute of Standards and Technology, Gaithersburg, MD 20899

<sup>2</sup>Mail Stop 500-115, NASA Lewis Research Center, Cleveland, OH 44135

## INTRODUCTION

In the inhabited quarters of orbiting spacecraft, fire is a greatly feared hazard. Thus, the fire safety strategy in a spacecraft is (1) to keep any fire as small as possible, (2) to detect any fire as early as possible, and (3) to extinguish any fire as quickly as possible. This suggests that a material which undergoes a momentary ignition might be tolerable but a material which permits a transition from a localized ignition to flame spread would significantly increase the fire hazard in a spacecraft. If the transition does not take place, fire growth does not occur. Therefore, it is critical to understand what process controls the transition.

Many previous works have studied ignition and flame spread separately<sup>1,2</sup> or were limited to a two-dimensional configuration<sup>3,4</sup>. In this study, time-dependent phenomena of the transition over a thermally thin sample is studied experimentally and theoretically in two- and three-dimensional (2D, 3D) configurations. Furthermore, localized ignition can be initiated at the center portion of thermally thin paper sample instead of at one end of the sample. Thus, the transition to flame spread could occur either toward upstream or downstream or both directions simultaneously with an external flow. In this presentation, the difference in the transition between the 3D and 2D configurations is explained with the numerically calculated data. For sufficiently narrow samples edge effects exist. Some results on this issue are presented. New analysis of the surface smoldering experiments conducted in the space shuttle STS-75 flight is also described.

## NUMERICAL RESULTS

The numerical model has been described in detail in our previous publication<sup>5,6</sup>. The theoretical prediction and the experimental data show that the transition from localized ignition to subsequent flame spread tends to occur more easily in the three-dimensional configuration than in the two-dimensional configuration in the oxygen supply limit regime such as a low external flow<sup>7</sup>. This trend is explained in Figure 1 (3D case) which shows the top down view of the stream lines and the mass flux vectors for both oxygen and fuel in the plane parallel to the sample surface. The colors used in the figures correspond to gas phase reaction rate. Pyrolysis and expansion from the gas phase reaction create an obstacle which the upstream originating flow circumvents. The upper and lower halves of the figure contain the fuel and oxygen mass flux vectors, respectively. Fuel gases flow radially from the center due to diffusion and expansion. Far from the flame, the oxygen mass flux vectors and streamlines point in the same direction (convective flux dominates). Oxygen mass flux along the outer regions of the flame is toward the centerline plane. The magnitude of the oxygen mass flux from the side (which is diffusion dominated) is as large or larger than the centerline flux in the upstream part of the flame (where it is most aided by the external flow). Diffusion in the 2D case can only occur within the centerline plane. Thus, it is clear that the curvature of the reaction zone of the 3D flame allows more oxygen to be supplied to the flame. The 3D flame is therefore less dependent on oxygen supply from an external flow and successfully undergoes transition to flame spread while the 2D flame is quenched (at this low external flow speed,

1 cm/s). More detail of this discussion can be found in our recent publication<sup>8</sup>.

In the experimental apparatus, a paper sample is secured within a stainless steel card. This card acts as a heat sink. For samples of a small enough width heat loss to the steel will affect flame evolution – even in the centerline plane which is farthest from the sample/steel interface. In such cases, a 2D model of the flame will not be accurate. Three 3D cases are simulated: 2 cm and 9 cm wide samples in stainless steel cards; and a 2 cm wide sample in a card with thermal properties identical to the sample. Figure 2 shows that the 2 cm wide sample cases differ significantly from each other and from the 9 cm wide case. Thus, edge effects significantly influence flame behavior in the centerline plane for the 2 cm wide samples. Figure 3 shows color contours of temperature on a reaction isosurface for the cases with a stainless steel card. The 2 cm case has a flame in the centerline plane which is smaller (consistent with Fig. 2), lower, and cooler. This is due to stronger diffusive mixing of oxygen from the outer region of the 2 cm wide flame (a 3D effect) as was seen in Fig. 1.

## EXPERIMENTAL RESULTS: SMOLDERING

The same type of the paper used for above flaming study was doped with potassium ions to enhance char formation and char oxidation and the experiments were conducted in air. Smoldering was initiated at the center of the sample by a lamp. Smolder patterns developing under two different gravity environments are shown in Figure 4. In normal gravity, as shown in Figures 4a-c, the glowing smolder front remained symmetric although segmented (horizontal sample in a quiescent condition). The smolder area pattern was nearly uniform and continuous. In microgravity, a very complex finger-shaped char pattern was observed from the onset of smoldering ignition. Discrete glowing smoldering fronts were localized at the finger tips as seen in Figures 4d-f (flow velocity of 0.5 cm/s). The direction of growth of the char fingers was almost solely upstream during the lowest flow velocity experiment. Normalized smolder area, a fraction of the upstream area available that smoldered, linearly increased with external flow, and approached unity (uniform front) at external flow velocities of 9 cm/s to 10 cm/s. Analysis of oxygen transport revealed that each smolder front cast an “oxygen shadow” which influenced the oxygen mass flux to adjacent smolder fronts. More detailed discussion can be seen in our recent publication<sup>9</sup>

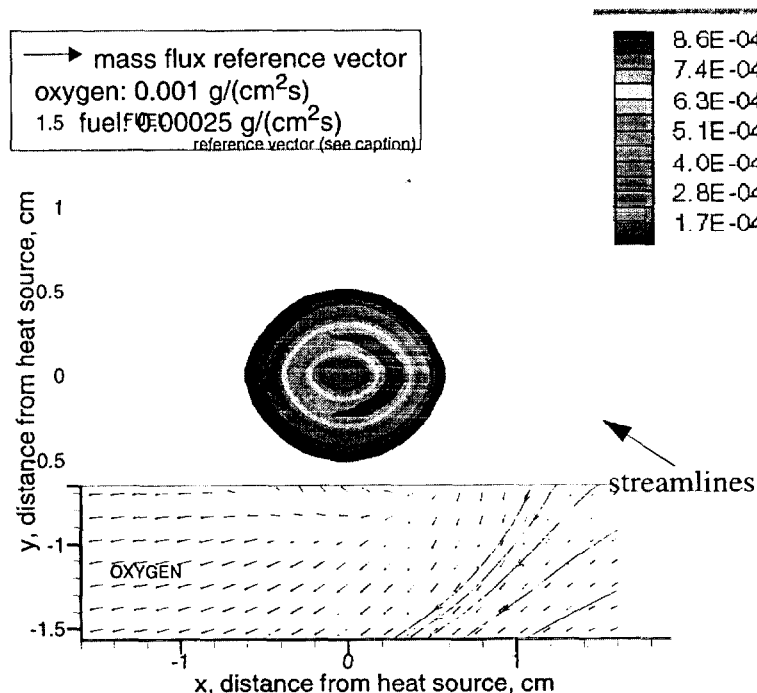
## ACKNOWLEDGMENTS

This study is supported by the NASA Microgravity Science Program under the Inter-Agency Agreement No.C-32001-R.

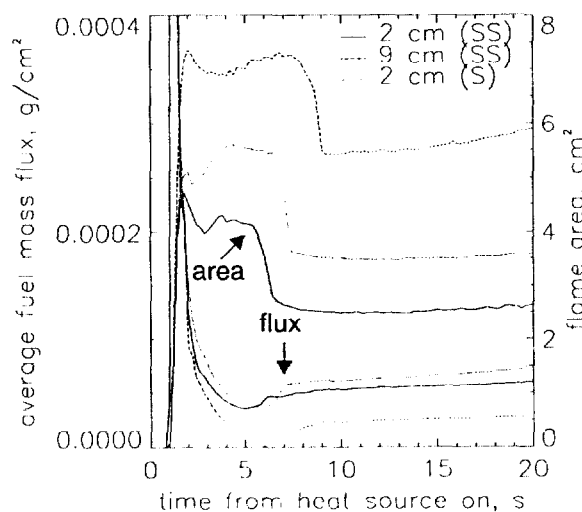
## REFERENCES

1. Amos, B. and Fernandez-Pello, A.C., *Combust. Sci. Tech.* 62:331-343 (1988).
2. Ferkul, P.V. and Tien, J.S., *Combust. Sci. Tech.* 99:345-370 (1994).
3. West, J., Tang, L., Altenkirch, R.A., Bhattacharje, S., Sacksteder, K., and Delichatsios, M.A., Twenty-Sixth Symposium (International) on Combustion, The Combustion Institute, pp.1335-1343 (1996).
4. Di Blasi, C., *Fire & Materials*, 22:95-101 (1998).
5. McGrattan, K.B., Kashiwagi, T., Baum, H.R., and Olson, S.L., *Combust. Flame* 106:377-391 (1996).
6. Kashiwagi, T., McGrattan, K.B., Olson, S.L., Fujita, O., Kikuchi, M., and Ito, K., Twenty-Sixth Symposium (International) on Combustion, The Combustion Institute, pp.1345-1352 (1996).

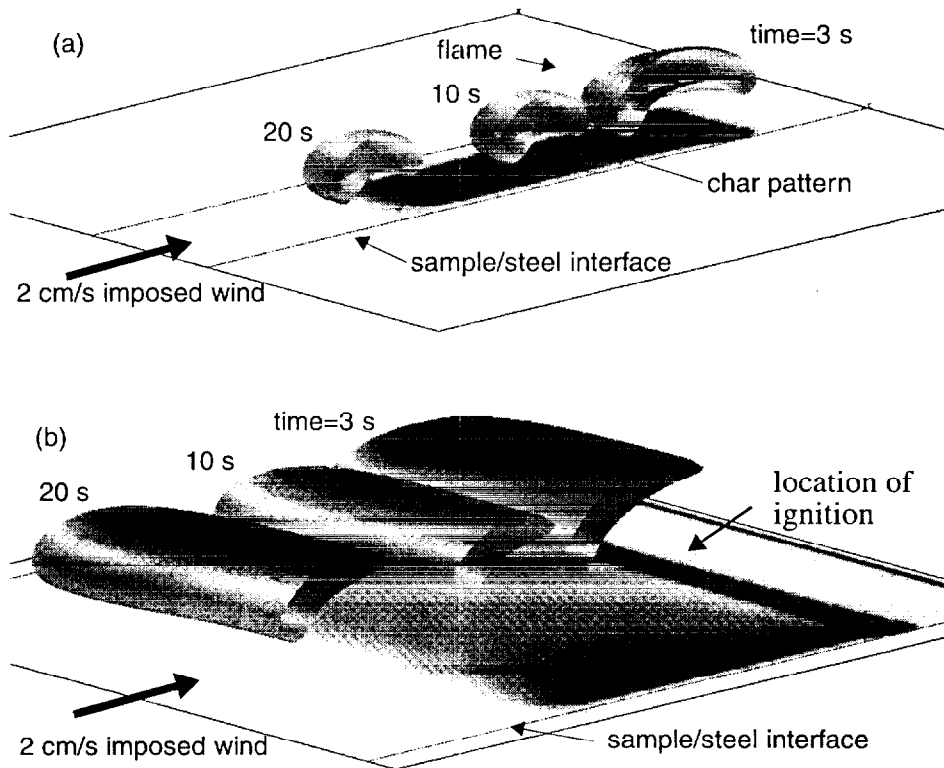
7. Kashiwagi, T., Mell, W.E., McGrattan, K.B., Baum, H.R., Olson, S.L., Fujita, O., Kikuchi, M., and Ito, K., Fourth International Microgravity Combustion Workshop, NASA Conference Publication 10194, p. 411-416 (1997).
8. Mell, W.E. and Kashiwagi, T., "Dimensional Effects on the Transition from Ignition to Flame Spread in Microgravity" in press, Twenty-Seventh Symposium (International) on Combustion, The Combustion Institute.
9. Olson, S.L., Baum, H.R., and Kashiwagi, T., "Finger-Like Smoldering Over Thin Cellulosic Sheets in Microgravity", in press, Twenty-Seventh Symposium (International) on Combustion, The Combustion Institute.



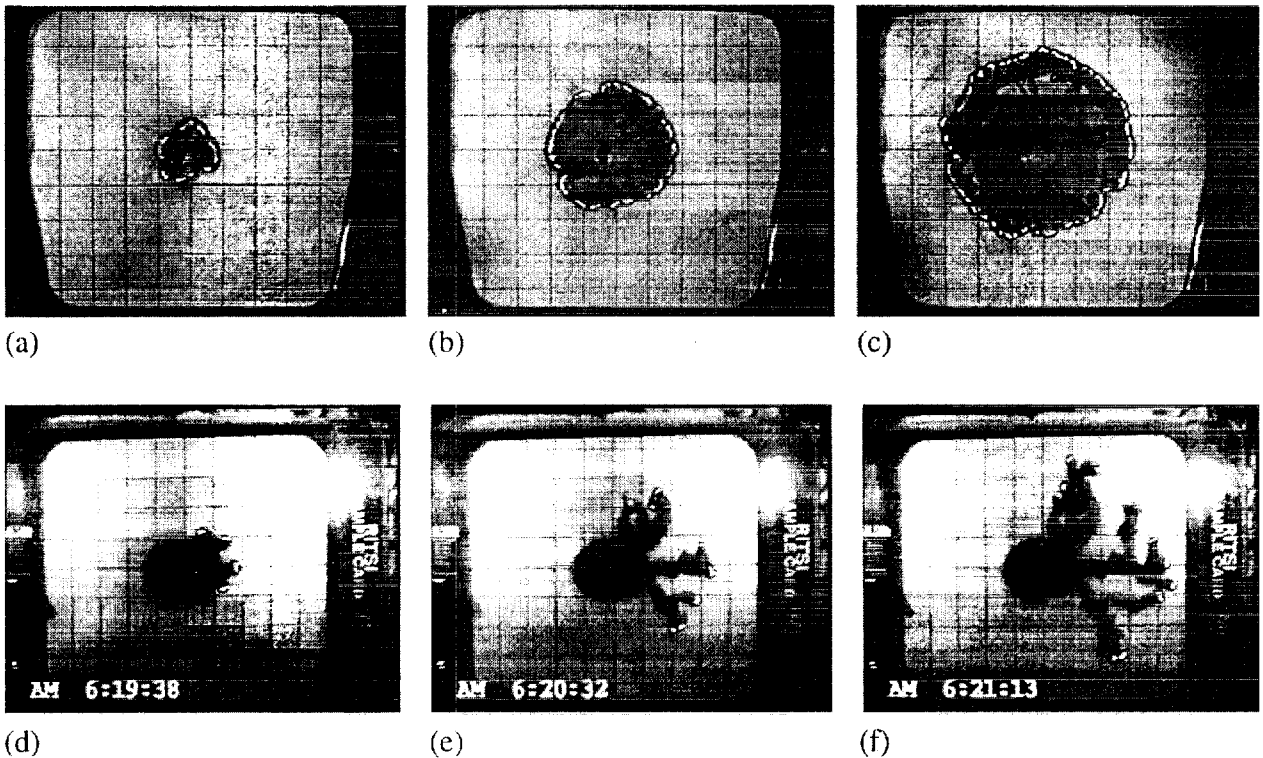
**Figure 1:** Various data on a horizontal plane 2.5 mm above the surface of a burning sample. Color contours of reaction rate ( $\text{g}/\text{cm}^3 \cdot \text{s}$ ), mass flux vectors (fuel on upper half, oxygen on lower half), and streamlines. A 1 cm/s wind flows from right to left. The flame is ignited by applying a radiative flux for 3.5 s to the paper over a circular area. The data shown here are at  $t=1.5$  s, shortly after ignition.



**Figure 2:** Average fuel mass flux from sample surface along the centerline and flame area in the centerline plane versus time. Three cases are shown: 2 cm and 9 cm wide samples bounded by stainless steel (denoted SS) and a 2 cm wide sample bounded by a non-degrading material with thermal properties identical to the sample (denoted S). Ignition occurs by applying a radiative flux across the width of the sample for 3.5 s (see Fig. 3). After approximately 10 s all flames are relatively quasi-steady. The fuel mass flux is directly related to the net heat flux on the sample. The flame area is largest in the 9 cm case but the fuel mass flux is smallest. This is because the 9 cm flame stands off the sample more – see Fig. 3. Flame area was computed by averaging all area elements in the centerline plane with reaction rates larger than  $1 \mu\text{g}/(\text{cm}^3 \cdot \text{s})$ .



**Figure 3:** Color contours of temperature on the  $50 \mu\text{g}/(\text{cm}^3 \cdot \text{s})$  reaction rate isosurface. Highest temperatures are in red; lowest in blue. Charring of the sample at  $t = 20 \text{ s}$  is denoted by greyscale. Three times  $t = 3 \text{ s}$ ,  $10 \text{ s}$ ,  $20 \text{ s}$  for two cases are shown: (a) 2 cm wide sample; (b) 9 cm wide. Overall dimensions are 11 cm length in wind direction, 10 cm wide.



Smolder patterns developing under conditions of normal gravity (a) - (c) and microgravity (d) - (f). In the microgravity case a  $0.5 \text{ cm/s}$  wind flows from right to left.